XLVI CILAMCE
VITÓRIA - ES - BRAZIL - 2025
XLVI IBERO-LATIN AMERICAN CONGRESS ON COMPUTATIONAL METHODS IN ENGINEERING

PARAMETRIC ANALYSIS OF FLOW IN A VERTICAL POROUS CHANNEL WITH MULTIPLE FRACTURES

Lucas V. Dias[1], Ana C. Caetano[1], Sergio Y. J. Ogata[2], Bruno F. Porto[1], Felipe de S. Bertola[1], Silvio L. M. Junqueira[2], Alex T. A. Waldmann[3], André L. Martins[3].

[1]Instituto SENAI de inovação em Engenharia de Estruturas
Rua José Correa de Aguiar, 361, Jardim Leblon, 87053-276, Maringá - PR, Brasil
lucas.vinicius@sistemafiep.org.br, ana.caetano@sistemafiep.org.br, bruno.porto@sistemafiep.org.br, felipe.souza@sistemafiep.org.br
[2]Centro de Pesquisas em Reologia e Fluidos Não Newtonianos, Universidade Tecnológica Federal do Paraná
Rua Dep. Heitor Alencar Furtado, 5000 - Campina do Siqueira, 81280-340, Curitiba - PR, Brasil
sergioyogatajr@gmail.com, silvio@utfpr.edu.br
[3]Centro de Pesquisas Leopoldo Américo Miguez de Mello
Avenida Horácio Macedo, 250, Cidade Universitária, 21941-915, Rio de Janeiro - RJ, Brasil
awaldmann@petrobras.com.br, aleibsohn@petrobras.com.br

Abstract. During the drilling of oil wells, the flow of drilling fluids through the annular space is affected by discontinuities and high-permeability regions in the geological formation, causing lost circulation, which reduces operational efficiency and compromises well integrity. To prevent this, selecting a drilling fluid suitable for the drilling phase and well characteristics is essential. This study develops a methodology to perform numerous simulations with varying input parameters to investigate lost circulation of a non-Newtonian fluid modeled by the power-law in a partially porous and fractured vertical channel. Fracture spacing and thickness variations are considered. Numerical simulations using CFD analyzed velocity profiles, pressure behavior, and loss percentage. The flow is assumed steady, incompressible, with flow in the free channel and fractures governed by Navier-Stokes equations, and flow in the porous medium described by the generalized equation by Vafai and Tien. Simulations were performed in OpenFOAM with porosity 0.7 and permeability 10^{-6} m². The fluid has consistency index k = 0.205 Pa·s^n , power-law index n = 0.568, density 1012.60 kg/m³, and the flow operates at Reynolds number Re = 1000. Python automation was implemented to run simulations and automate post-processing, optimizing execution time and enabling systematic analysis of multiple scenarios for better understanding of system behavior.

Keywords: Lost circulation, Partially Porous Fractured Channel, OpenFOAM, Discrete fractures.

1 Introduction

During the oil well drilling process, the circulation of drilling fluid — essential for stabilizing the wellbore, preventing formation influxes, providing geological data, and removing cuttings generated at the bottom of the well — can be disrupted by geological discontinuities such as cavernous formations, fractures, and highly permeable zones [1]. Lost circulation (LC) occurs when the drilling fluid invades the geological formation due to the wellbore pressure exceeding the formation pore pressure. Lost circulation accounts for 10% to 20% of the total drilling costs due to loss of materials and non-productive time, in addition to increasing operational risks [2].

Given this scenario, numerical simulations were performed considering the flow of non-Newtonian fluids, whose viscosity varies with the shear rate [1] and which, in this work, was described by the Power-Law model. For this purpose, the well geometry was simplified using Cartesian coordinates, inspired by previous studies such as Ogata [3], Schneider [4], and Andreatta [5], allowing the representation of the annular region and the permeable formation with transverse fractures for fluid-porous flow analysis.

According to Vafai and Tien [6], the flow in the free-flow regions and fractures can be described by the Navier–Stokes equations, while in the high-permeability porous medium a continuum formulation is applied that

considers viscous, drag, and inertial effects. The numerical solution was obtained using the finite volume method implemented in OpenFOAM 24.06, with adaptations in the porousSimpleFoam solver, including viscous diffusion effects in addition to linear and inertial drag terms.

Therefore, the objective of this study is to create a methodology to execute a large number of simulations with varying input parameters to investigate lost circulation of a non-Newtonian fluid described by the Power-Law model in a partially porous and fractured channel geometry, considering variations in fracture spacing and thickness. Numerical simulations with multiple parameter combinations were conducted to analyze velocity profiles, pressure behavior, and loss percentage. To optimize execution time, Python automation was implemented to run the simulations sequentially, as well as to post processing the data, enabling a systematic analysis of the simulated scenarios and contributing to a better understanding of the system's behavior.

2 Problem Formulation

This work is based on the model by Andreatta [5], who numerically simulated the flow in a partially porous channel with multiple fractures. In the present study, the well geometry was simplified using Cartesian coordinates, considering a section of the annular region and the permeable formation with transverse fractures, as illustrated in Figure 1. The boundary conditions adopted, with zero pressure at the outlets of the fractures and the vertical channel, create preferential flow paths, as proposed by Andreatta.

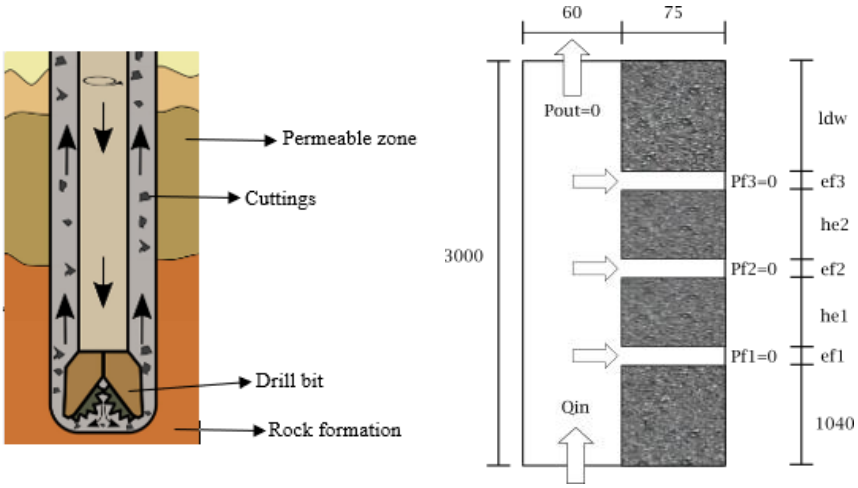


Figure 1: Original cylindrical well and rock formation model (left), adapted from [3], and the simplified well geometry used in this study (right).

As illustrated in Figure 1, the following variables are defined: $Pout$ represents the outlet pressure in the vertical channel; Qin is the inlet flow rate; Pf denotes the pressure at the fracture outlet; ef corresponds to the fracture thickness; he indicates the height between fractures; and ldw is the height from above the fractures to the end of the vertical channel.

To execute parametric simulations, a Python script was developed to fully automate the workflow in OpenFOAM. This automation included generating all combinations of input parameters, dynamically modifying the case files, running the solver, monitoring the simulation logs, handling exceptions, and exporting and saving the results.

The fluid flow was modeled using the mass and momentum conservation equations (Equations 1 and 2). Assuming an isothermal, incompressible, and steady-state flow in a Cartesian system, the governing equations are represented as [7]:

$$\vec{\nabla} \bullet \vec{u} = 0 \tag{1}$$

$$\rho \vec{\nabla} \bullet (\vec{u}\vec{u}) = -\vec{\nabla} p + \vec{\nabla} \bullet \tau \tag{2}$$

where ρ $[kg \cdot m^{-3}]$ is the fluid density, τ $[Pa]$ is the shear stress tensor, u $[m \cdot s^{-1}]$ is the velocity vector, and p $[Pa]$ is the pressure field.

Non-Newtonian fluids exhibit an apparent viscosity that depends on the shear rate $\dot{\gamma}yx$ $[s^{-1}]$. For Power-Law (PL) fluids, two parameters are defined: the consistency index k $[Pa \cdot s^{n}]$ and the flow behavior index n. The constitutive equation for a PL fluid is given by Chhabra [8]:

$$\mu_{lp} = \frac{\tau_{yx}}{\dot{\gamma}_{yx}} = k\left(\dot{\gamma}_{yx}\right)^{n-1} \tag{3}$$

The flow in the homogeneous porous medium (PM) is described by the Darcy–Brinkmann–Dupuit–Forchheimmer (DBDF) equation, as presented by Lage [9]:

$$\frac{\rho_f}{\varepsilon^2}\vec{\nabla}\bullet(\vec{u}\vec{u}) = -\vec{\nabla}p + \frac{\mu}{\varepsilon}\vec{\nabla}\bullet\tau - \left(\vec{u}\frac{\mu}{K} + CF\vec{u}|\vec{u}|\frac{\rho_f}{\sqrt{K}}\right), \text{ where } CF = \frac{1{,}75}{\sqrt{150 * \varepsilon^3}} \tag{4}$$

Where K [m²] is the absolute permeability, ρ_f is the fluid density, ε is the porosity (volume fraction), and CF is the dimensionless drag coefficient, which represents the additional resistance to flow caused by the porous medium's structure. The values 1.75 and 150 are empirical parameters from Ergun's correlation [10], used to quantify the drag due to the geometry and distribution of pores in the medium, accounting for friction and inertial effects as the fluid flows through the porous matrix.

2.1 Numerical formulation

The conservation equations were discretized using the Finite Volume Method, with the SIMPLE algorithm (Semi-Implicit Method for Pressure-Linked Equations) employed for pressure-velocity coupling. Simulations were performed with non-uniform structured meshes, featuring local refinement in regions with high gradients, such as walls and fluid-porous interfaces.

The open-source software used was OpenFOAM 24.06, which includes the native solver porousSimpleFoam. This solver implements the Darcy-Forchheimmer resistance model for porous media, based on the following formulation:

$$\rho\vec{\nabla}\bullet(\vec{u}\vec{u}) = -\vec{\nabla}p + \mu\vec{\nabla}\bullet\tau + \overrightarrow{S_i} \tag{5}$$

$$\overrightarrow{S_i} = -\left(\vec{u}\mu D + F\vec{u}|\vec{u}|\frac{\rho}{2}\right) \tag{6}$$

Where S_i is the volumetric resistance force, $D = 1/K$ is the linear (Darcy) contribution, and F is the non-linear drag coefficient contribution (Forchheimmer), defined as:

$$F = 2 * \mathrm{CF} \tag{7}$$

Although porousSimpleFoam implements the Darcy–Forchheimmer model, it does not account for porosity effects in the convective and diffusive terms of the momentum equation, as required by the full Darcy–Brinkmann–Dupuit–Forchheimmer (DBDF) model described in Equation (4). Therefore, a customized solver was developed based on this code, incorporating corrections to the advective term (divided by ε^2) and the diffusive term (divided by ε), as well as reformulating the source term using the drag coefficient, according to Ergun's correlation. These modifications provide a more accurate representation of flow in homogeneous porous media.

2.2 Verification Test

To verify the implementation of the solver in OpenFOAM, validation was performed by simulating the flow problem proposed for the analysis of NNF flow, the case of Silva [11], where the fluid moves through a space bounded by two porous plates and free fluid region in the middle with a developed velocity profile. Along a vertical line perpendicular to the flow, the dimensionless velocity profile from wall to symmetry axis was plotted in 2, for comparison.

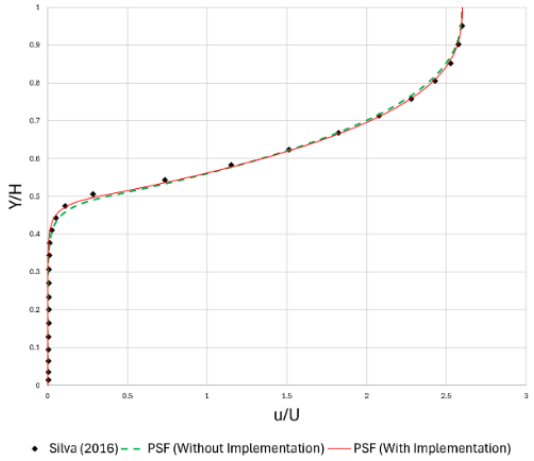


Figure 2. Comparison between the analytical and numerical solutions of the dimensionless velocity profile of flow between parallel plates with porous layers for Re=100, n=0.60, ε=0.60, and Da=1e-06.

In this, it is also possible to observe a significant difference in the implementation of the solver for flow in PM, with a smaller relative error with the implementation, and a qualitative behavior more like that presented by the literature.

Thus, the correction of advective and convective terms in the momentum equation for porous medium was necessary to reproduce physics properly to reproduce more accurate results for the proposed problem in present work.

2.3 Results

In this study, the NNF is characterized by a density of $1012.60\ kg \cdot m^{-3}$, a consistency index k of $0.205\ Pa \cdot s^n$, and a flow behavior index n of 0.568. The simulations were conducted considering a Reynolds number of $Re = 1000$, porosity $\varepsilon = 0.75$, and permeability $K = 10^{-6}\ m^2$. A total of 243 parametric simulations were performed by varying the distance between fractures (he = 100, 200, and 400 mm) and the fracture thickness (ef = 4, 16, and 40 mm).

A total of 243 simulations were performed, each with 2000 iterations. This number was defined based on the stabilization of pressure and velocity residuals, whose variations remained below 5%, indicating a plateau in the results. The average time per iteration was 6.7 seconds.

Table 1 – Simulation Performance: Iterations and Average Time

Total Simulations	Total Execution Time (days)	Number of Iterations per Simulation	Average Execution Time per Simulation (h)	Average Execution Time per Simulation (s)	Time per Iteration (s)
243	38	2000	3,72	13406	6,7

Based on the simulation results, the effect of fracture thickness and the distance between them on accumulated circulation loss was observed. Fractures 4 mm thick, regardless of position and/or order, present the lowest fluid losses, accounting for values in the 1% range even when three fractures with 4 mm thicknesses are located close to each other.

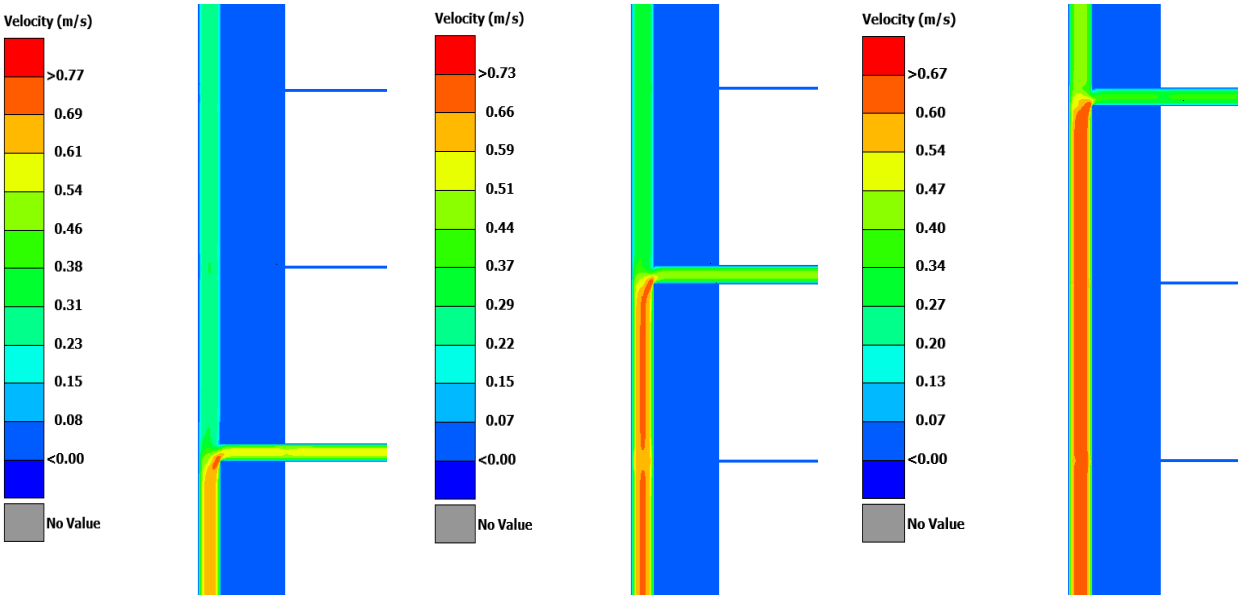
Analyzing each fracture individually, the statistical metrics for circulation loss per fracture can be seen in Table 2.

Table 2 – Descriptive Statistics of Lost Circulation in a Partially Porous Channel with Three Fractures

	4 mm	16 mm	40 mm
Mean	0.25%	13.49%	44.53%
Minimum	0.14%	7.82%	31.20%
Maximum	0.39%	19.10%	54.88%
Range	0.25%	11.28%	23.68%
Standard Deviation	0.06%	2.81%	5.88%
Variance	0.00004%	0.08%	0.35%

For the 4 mm fractures, the average loss was 0.25%, with a maximum accumulated loss of 1.05% and a maximum individual value of 0.39%. The lowest total loss (0.96%) was obtained from a configuration where three 4 mm fractures were spaced 400 mm apart. The lowest unit loss (0.14%) occurred in a setup with more than two 40 mm fractures.

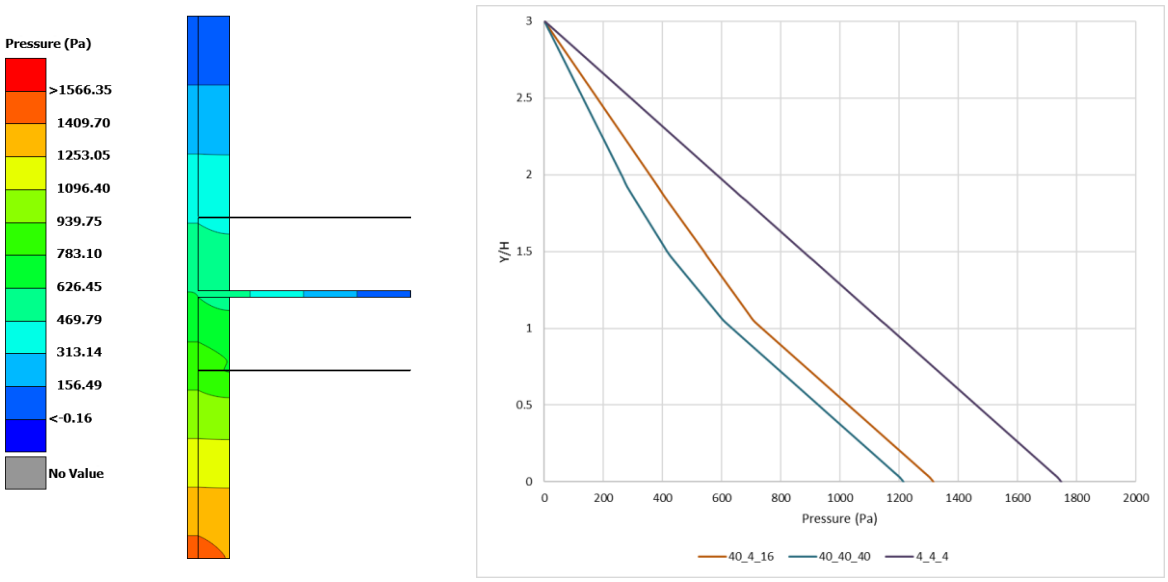
Similarly, an analysis was performed with three 40 mm fractures, yielding the highest losses, with an average loss of 37.44% per fracture in these configurations, and an average loss of 44.53% per fracture when considering all possible combinations. The maximum value per fracture occurs when the thickness is 40 mm followed by two 4 mm fractures. Figure 3 shows the distribution of flow velocities in the 4 and 40 mm fractures.



40mm-4mm-4mm (a) 4mm-40mm-4mm (b) 4mm-4mm-40mm (c)

Figure 3. Loss Distribution in 4 mm and 40 mm Fracture Schemes

Analyzing the pressure profile, it is possible to observe that although greater pressure is required to overcome the vertical column when the fracture is further from the inlet, the profiles qualitatively present similar behavior for the three configurations. The relaxation in pressure with the loss of fluid for the 4 mm fracture is almost insignificant in the flow itself, as can be seen in Figure 4 where the pressure profile becomes a straight line with a constant angle, while for the profile with 16 and 40 mm fractures there is a change in inclination when approaching the fractures



(a) (b)

Figure 4. Pressure distribution in the vertical channel (a) pressure profile for 4 mm, 40 mm and 4 mm fractures (b) pressure curves in the vertical channel for three fracture configurations.

Still on pressure, it was noticed that with the increase in the thickness of the fractures, the pressure at the inlet necessary for the flow to occur shows a tendency to decrease, since with the escape of the fluid there is a relaxation of the pressure in the vertical channel. This can be seen in Figure 5, where pressure was plotted alongside the percentage of circulation loss across the simulations performed (243 simulations in total).

The percentage of circulation loss was ordered in ascending order to visualize the limits of fracture losses, and the points at which the fracture thickness began to be used in the simulation were marked (Figure 5). It was important to note that with a thickness of 16 mm in the three fractures, their loss values were equivalent to the loss of one 40 mm fracture followed by two fractures with a thickness of 4 mm. Thus, since the 4 mm fractures mostly present a loss of a maximum of 0.39%, it is still possible to state that if a single 40 mm fracture were to occur in the partially porous channel, it would be equivalent to three 16 mm fractures with a spacing of 100 mm between each

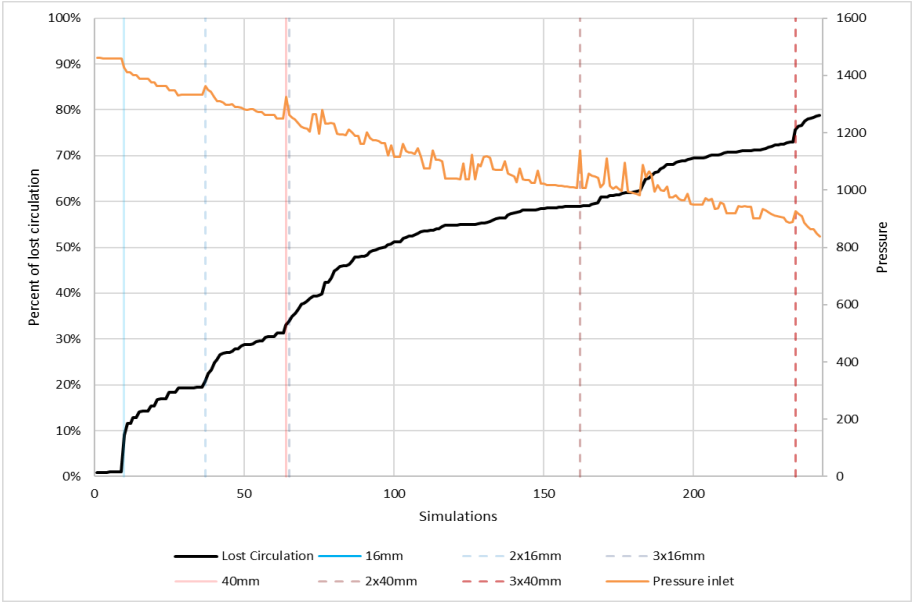


Figure 5. Percentage of circulation loss ordered in increasing order, together with its respective pressure at the channel inlet

It can also be seen in Figure 5 that 1.05% loss only occurs for fractures of up to 4 mm. Considering the minimum loss for fractures with a thickness of 16 mm of 7.82%, the first sign of this occurrence occurs at 9.12%,

where the loss is the result of two 4 mm fractures and one 16 mm fracture spaced 400 mm apart. The sign for the appearance of two 16 mm fractures is only at 20.33%, combined with one 4 mm fracture and 400 mm spacing.

The first 40 mm fracture appears at least 33.05%, and as already mentioned, competes with the formation of three 16 mm thicknesses. Starting at 39.86%, it is possible to establish that a 40 mm fracture is necessarily present in the combinations, followed by two fractures at 59% and three necessarily after 75.71% material loss.

3 Conclusion

In this study, the phenomenon of lost circulation of non-Newtonian power-law fluids in partially porous and multiple fractured channels was numerically investigated using OpenFOAM 24.06, with a solver modified from porousSimpleFoam. The modeling incorporated the effects of porosity in the convective and diffusive terms of the momentum equations, as required by the non-linear drag coefficient contribution.

A total of 243 parametric simulations, managed by the Python automation script, were conducted, enabling a detailed analysis of the influence of fracture thickness and spacing on the magnitude of lost circulation. The results showed that thinner fractures (4 mm), regardless of configuration, resulted in the lowest loss rates (average of 0.25% and maximum of 1.05%), while thicker fractures (40 mm) led to significant losses (average of 44.53%, maximum of 54.88%).

It was observed that three 16 mm fractures with reduced spacing (100 mm) can cause losses equivalent to those of a single 40 mm fracture, highlighting the importance of the relative positioning of discontinuities. A hierarchy of fracture configurations in terms of their impact on LC was also established, which can serve as technical support for drilling fluid selection and operational planning to mitigate losses in real wells.

The proposed methodology, based on numerical simulation coupled with Python scripting automation, proved to be a robust and efficient tool for large-scale parametric analysis. The results reinforce the relevance of CFD modeling as a predictive tool for controlling operational issues during drilling, contributing to cost reduction and increased safety in the oil and gas sector.

Acknowledgements. The authors would like to express their gratitude to the Financiadora de Estudos e Projetos (FINEP) for their financial support of this project, under the contract code 01.24.0263.00. The authors are grateful to the Brazilian Petroleum Agency (ANP), the Human Resources Program for the Petroleum and Gas Sector PRH-ANP (PRH21.1 - UTFPR), and CENPES-PETROBRAS for the provided financial support.

Authorship statement. The authors hereby confirm that they are the sole liable persons responsible for the authorship of this work, and that all material that has been herein included as part of the present paper is either the property (and authorship) of the authors, or has the permission of the owners to be included here.

References

[1] BOURGOYNE JR, A. T.; MILLHEIM, K. K.; CHENEVERT, M. E.; YOUNG JR, F. S. Applied drilling engineering. Volume 2. 1991.

[2] COOK, J.; GROWCOCK, F.; GUO, G.; HODDER, M.; VAN OORT, E., 2012. “Stabilizing the Wellbore to Prevent Lost Circulation,” Oilfield Review, v. 23, n. 4, p. 26–35.

[3] OGATA , S. Y. (2021). Estudo numérico da perda de circulação com fluido de lei de potência em canal parcialmente poroso e fraturado. Trabalho de Conclusão de Curso, Bacharelado em Engenharia Mecânica, Departamento Acadêmico de Mecânica, Universidade Tecnológica Federal do Paraná. Curitiba.

[4] SCHNEIDER, C. L., DE LAI F. C., WALDMANN, A. T. A., MARTINS A. L., JUNQUEIRA, S. L. M. (2019), "Experimental study of lost circulation of non newtonian fluids in fractured proorous media", VIII Encontro Nacional de Construção de Poços de Petróleo e Gás (ENAHPE), Serra Negra - SP.

[5] NDREATTA, L. V. R. (2011), Escoamento em canal parcialmente poroso e fraturado. UTFPR – Curitiba – PR, 133p. (projeto de final de curso).

[6] VAFAI, KAMBIZ; TIEN, CHANG L. Boundary and inertia effects on flow and heat transfer in porous media. International Journal of Heat and Mass Transfer, v. 24, n. 2, p. 195-203, 1981.

[7] PRITCHARD, P. J., LEYLEGIAN, J. C., Fox and McDonald’s Introduction to Fluid Mechanics. 8 th edition, John Wiley Sons, Inc., 2011.

[8] CHHABRA R. P., RICHARDSON, J. F. Non-Newtonian flow in the process industries. 1st edition, Butterworth-Heinemann, Woburn, MA, 1999.

[9] LAGE, J. L. “The Fundamental Theory of Flow Through Permeable Media from Darcy to Turbulence,” in Transport Phenomena in Porous Media, edited by D. B. Ingham and I. Pop, Pergamon/Elsevier, 1998.

[10] ERGUN, S. Fluid Flow through Packed Columns. Chemical Engineering Process, vol. 48, pp. 89-94, 1952

[11] SILVA, R.A.; ASSATO. M.; DE LEMOS, M.J.S. Mathematical modeling and numerical results of power-law fluid flow over a finite porous medium. International Journal of Thermal Sciences; vol. 100, pp. 126-137, 2016.